

# Comparison of Human Head Phantoms with Different Complexities for Implantable Antenna Development

Shubin Ma, Leena Ukkonen, Lauri Sydänheimo, Toni Björninen  
 BioMediTech Institute and Faculty of Biomedical Sciences and Engineering  
 Tampere University of Technology  
 Tampere, Finland  
 {shubin.ma, leena.ukkonen, lauri.sydanheimo, toni.bjorninen}@tut.fi

**Abstract**— Human body phantom with electrical properties is widely used in electromagnetics solvers to model the lossy human tissue environment. The selection of the phantoms affects the computational efficiency and results accuracy. In this work, we evaluated four human head phantoms with an intracranial implantable antenna. Results of phantom complexity and antenna parameters are compared to provide the reference in phantom selection for implantable antenna development.

**Keywords**— implantable antenna, multilayer head phantom, anatomical head phantom.

## I. INTRODUCTION

Implantable wireless devices play a significant role in the future telemedicine and remote vital-sign monitoring system, as they substitute the cable for in-to-out body wireless communication links. However, the inhomogeneous human tissues with high permittivity and notable conductivity bring the unpredictable degradation to the radio link in the proximity of it. The full-wave EM (electromagnetic) simulator is an effective tool to investigate this human tissue impact on EM performance of the implantable devices. In the simulator, human body phantom with tissue electrical properties is widely used to mimic the lossy tissue environment. In the literature, different approaches to constructing the phantom have been proposed, from the simple geometric shape based to the complex medical images based ones. With the increase of the phantom complexity, more details of the tissue geometrical information can be retained, but the consumption of computational resource raises in the EM simulator. Therefore, block phantom constructed based on the predominant human tissues are widely used to improve the computational efficiency. The main concern of using these simplified models is their lack of capability to reflect sufficient tissue characteristics from the perspective of EM wave propagation. This work aims to compare the reliability of a layered ellipsoid semi-anatomical human head model with the medical image based anatomical head model and a layered block model. The through-body radio link is established with a spatially distributed UHF RFID antenna developed from our previous work [1]. Fig.1 shows the head models and the implantable antenna with its geometrical dimensions.

## II. SIMULATION SETUP

### A. Antenna System

The antenna system involved in the human model evaluation consists of a wearable and an implant parts. The implant part is assumed to be in contact with the CSF

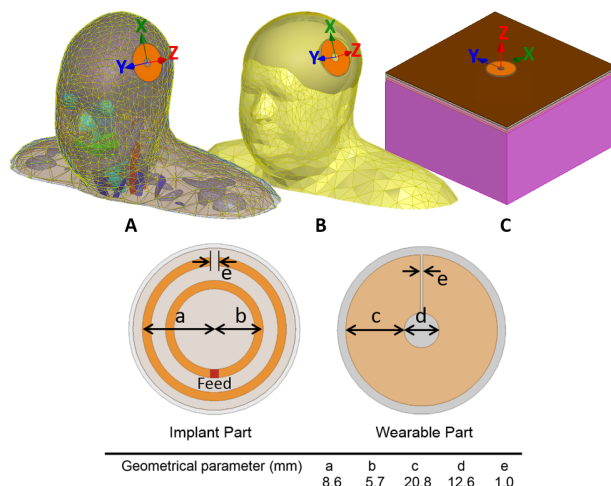


Fig. 1. Human head models and the implantable antenna with its geometrical dimensions

(cerebrospinal fluid) and that wearable part is concentrically placed on the scalp. The substrates for the wearable and implant parts are 2 mm thick EPDM (Ethylene-Propylene-Diene-Monomer) ( $\epsilon_r=1.26$ ,  $\tan\delta=0.007$  at 915 MHz) and 50  $\mu\text{m}$  thick flexible polyethylene ( $\epsilon_r=2.25$ ,  $\tan\delta=0.001$  at 915 MHz), respectively. The coating material for the implant part is the 1 mm thick silicone ( $\epsilon_r=2.2$ ,  $\tan\delta=0.007$  at 915 MHz). The RFID microchip in the simulation is modelled by the parallel connection of the resistance and capacitance of 2.85 k $\Omega$  and 0.91 pF, respectively. The antenna impedance is optimized to be complex-conjugate matched with the microchip in the CSF environment.

### B. Antenna Performance Indicators

The attainable read range ( $d_{tag}$ ) given in (1) is the main indicator to compare the system performance in different head models.

$$d_{tag} = \frac{\lambda}{4\pi} \sqrt{\frac{De_r\tau EIRP}{P_{ic0}}}, \quad \text{where } \tau = \frac{4\text{Re}(Z_A)\text{Re}(Z_C)}{|Z_A+Z_C|^2} \quad (1)$$

The  $d_{tag}$  is in inverse proportion to RFID IC wake-up power ( $P_{ic0}$ ) and proportional to antenna directivity ( $D$ ), radiation efficiency ( $e_r$ ), power transfer efficiency ( $\tau$ ), and the equivalent isotropically radiated power limitation ( $EIRP$ ). The  $\tau$  measures the portion of the power delivered from the antenna to the IC relative to the maximum power available from the antenna. In

other words, the factor  $0 < \tau \leq 1$  quantifies the goodness of the complex conjugate impedance matching between the antenna and the IC. Obviously, the  $D$ ,  $e_r$  and  $\tau$  directly influence the  $d_{tag}$  and thus these antenna parameters will be respectively evaluated in the simulation.

### C. Human Head Models

The anatomical head model shown in Fig.1 (A) is derived from the open source cryosection image based VHP-female model [2]. This head model has 15 individual tissues and 58 separate tissue parts. The semi-anatomical model illustrated in Fig.1 (B) is built by integrating a seven-layer ellipsoid to replace the cranial cavity of the VHP model. Its layered structure was constructed as ellipsoid shells with an adjustable thickness representing skin, fat, muscle, skull, CSF (cerebrospinal fluid) and brain (grey matter). The thickness of each layer is assigned with the corresponding tissue thickness measured from the implant location of the VHP model. The total distance between the antenna implant part and wearable part is 14 mm. Fig.1 (C) depicts the block model with a dimension of 30 mm  $\times$  30 mm  $\times$  20 mm. It has the identical 6-layer structure as that of the ellipsoid one but all the layers are in a flat form. The electrical properties assigned to each tissue in these models are obtained from IT'IS foundation. Additionally, to investigate the impact of the subsidiary tissues on the antenna EM performance, we reduced the VHP model to a simplified version with only six major tissue types: skin, fat, muscle, skull, CSF and brain.

## III. RESULTS AND DISCUSSION

We used finite element method based EM solver ANSYS HFSS v17 to compare the performance of each head model. The PC performed the simulations is equipped with Intel i7 X990 at 3.47 GHz with 24 GB of RAM. We monitored the convergence of the solution in each model in terms of the change in the parameters shown in Fig. 2 versus the mesh iterations. At the sixth iteration, the change in  $\tau$ ,  $e_r$ , and  $D$  had reduced to the maximum of 0.01%, 0.14% and 0.13%, respectively in all models and we considered these sufficient criteria for convergence. Table 1 lists the number of solved elements and the simulation time (mesh creation and solving 15 frequency points) in the different models. The time consumed in the VHP model with full tissue types is more than six times as that in the ellipsoid and block model. It is also noticeable that the simplification of the VHP model prominently reduces the model complexity and the time consumption.

Fig. 2 shows the simulated  $\tau$ ,  $e_r$ ,  $D$  and  $d_{tag}$  in the four head models. The VHP model with full tissue types is considered as the reference model in aid of evaluating the other three models. All the antenna far field parameters are calculated in the positive Z direction as denoted in Fig.1. According to Fig. 2(A), both the ellipsoid and block models have a detuning of the peak frequency from 925 MHz to 942MHz. Conversely, the

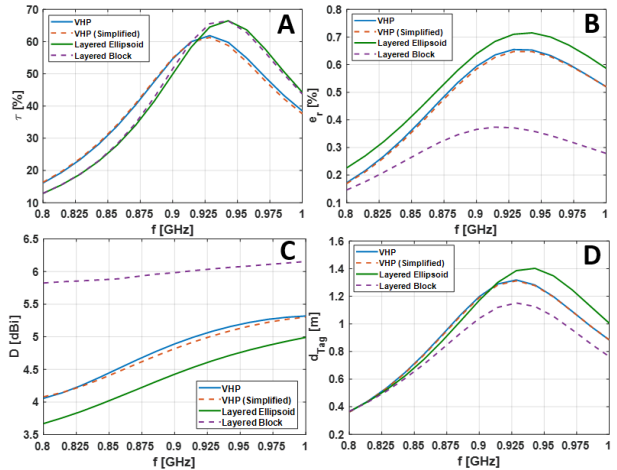


Fig. 2. Comparison of simulated  $\tau$ ,  $e_r$ ,  $D$  and  $d_{tag}$  of the four models.

simplified VHP model has a negligible impact on  $\tau$ . In terms of the  $e_r$ , as shown in Fig.2 (B), the block model has the worst performance with not only a peak frequency shift but also a clear 50% level underestimation, whereas, the ellipsoid model accurately estimates the peak frequency with less than 10% overestimation of the efficiency level. In the comparison of  $D$  shown in Fig.2 (C), the block model again fails to reflect its variation versus the frequency and a 1.5 dB level shift can be observed. The ellipsoid model, on the other hand, successfully characterizes the variation of  $D$  along with the frequency and level underestimation is less than 0.5 dB. Finally,  $d_{tag}$  simulated in the four models are shown in Fig.2 (D). Here the block model shows fair agreement with the others, but it should be noted that this agreement is only because of its poor predictions of  $e_r$  and  $D$  compensating each other in the computation of  $d_{tag}$ . The ellipsoid model shows a minor frequency detuning and level shift in  $d_{tag}$  compared with the VHP model, but provides a notable factor of 86% reduction in the simulation time. Simplified VHP model provides minimal deviation from VHP model and reduction by a factor of 63% in simulation time.

## IV. CONCLUSION

We compared four human head models for simulating an antenna system composed of an intracranial implant and head-worn parts. Our results show that antenna impedance can be estimated with a layered block model, but it fails to predict the antenna radiation field appropriately. A layered ellipsoid model predicts very similar impedance and estimates the far field parameters sufficiently well without increasing the simulation time. The two anatomical models: VHP and VHP (simplified) predict virtually the same antenna parameters that are also very close to those obtained from the ellipsoid model. Overall, the results support using the ellipsoid model for initial antenna optimization and robustness studies where the layer thicknesses are variable and the VHP (simplified) for final verifications.

## REFERENCES

- [1] S. Ma *et al.*, "Split ring resonator antenna system with implantable and wearable parts for far field readable backscattering implants," in Proc. IEEE AP-S Symp., 9–15 July 2017, San Diego, CA, USA, pp. 1689–1690.
- [2] J. Yanamadala *et al.*, "Multi-purpose VHP-female version 3.0 cross-platform computational human model," 2016 10th EuCAP, Davos, 2016, pp. 1–5

TABLE I  
SOLVED ELEMENTS AND TIME CONSUMPTION OF EACH MODEL

Model	Solved Elements	Time (min)
VHP	343,007	221
VHP (Simplified)	192,605	80
Layered Ellipsoid	130,497	29
Layered Block	143,958	33